Journal of Visualization, Vol. 6, No. 2 (2003) 95-106

Several Applications of Laser Diagnostics for Visualization of Combustion Phenomena

Chung, S. H.*

* School of Mechanical and Aerospace Engineering, Seoul National University, Seoul 151-742, Korea.

Received 25 September 2002
Revised 30 November 2002

Abstract : Several applications of laser diagnostic techniques to visualize combustion phenomena are presented, including reactive Mie scattering for flow, Rayleigh and Raman spectroscopy for major species, laser-induced fluorescence for minor species, and laser extinction, scattering, and laser-induced incandescence for soot. These techniques have been applied to diffusion flame oscillation, a recirculation zone in a burner, laminar and turbulent lifted flames, flame propagation along a vortex tube, and soot zone characteristics, to demonstrate the usefulness of the techniques to provide a better understanding of physical mechanisms.

Keywords : Visualization, Laser diagnostics, Lifted flame, Flame oscillation, Vortex, Soot.

1. Introduction

Combustion diagnostics techniques using lasers have advanced remarkably during the last two decades (Eckbreth, 1966) with the advent of powerful lasers, through which many combustion related physico-chemical mechanisms have been more clearly understood. Since the study of combustion involves chemically reacting flow with heat and mass transport, the phenomena associated with combustion is complicated. Consequently, conventional measurement techniques utilizing probes are often inadequate due to high temperature and spatial resolution problems, so that non-intrusive techniques using lasers are required.

In order to understand combustion phenomena, information on velocity, species concentration, and temperature are needed. Diagnostic tools are used to characterize and visualize the flow field and reaction zone in the study of combustion. The flow visualization techniques may include Mie scattering, reactive Mie scattering (RMS), and Rayleigh scattering, and the reaction visualization techniques may include Rayleigh and Raman scatterings, laser-induced fluorescence (LIF), light extinction/scattering (LE/LS) and laser induced incandescence (LII).

The objective of this paper is to present several applications of these techniques to various combustion phenomena. Therefore, the background physics of each diagnostic technique will not be addressed. Rather, we will state the areas that require investigation for each topic, the diagnostic techniques applied, and the information that can be gained using the technique. The visualization techniques include RMS, Rayleigh and Raman scatterings, LIF, LE/LS, and LII. These techniques

are applied in order to understand diffusion flame oscillations, flames in an axisymmetric curved-wall jet burner, flame stabilization in jets, flame propagation through vortex rings, and soot formation in diffusion flames.

2. Flow Visualization

2.1 Oscillating Diffusion Flames

A laminar diffusion flame stabilized on a burner rim could oscillate when the jet velocity is O (10 cm/s) and the nozzle diameter is O (1 cm). The oscillating frequency is about 12-14 Hz (Lee et al., 1998). In such a situation, a flame bulge appears along the flame surface (Fig. 1a), which migrates downstream periodically by the modified Kelvin-Helmholtz instability, due to the rapid acceleration near the central region caused by the buoyancy.

To clarify the mechanism of flame bulge formation, the reactive Mie scattering (RMS) technique has been applied, which collects Mie scattering signals from particles generated in the flow field. Chemically pure grade (>99%) propane is supplied from the center nozzle, which is surrounded by the coflow dry air. Trace amounts of titanium tetrachloride ($TiCl_4$) vapor was doped in the dry air. This vapor can react with water vapor and titanium oxide (TiO_2) particles are generated from the reaction of $TiCl_4 + 2\ H_2O \rightarrow TiO_2 + 4\ HCl$.

A sheet beam from a Nd:YAG laser (532 nm) was illuminated on the center plane. The corresponding scattering image is shown in Fig. 1b, demonstrating three scattering layers. The innermost layer that resembles the flame shape is from the Mie scattering by soot particles. The outermost layer is from the TiO_2 particles by the reaction with water vapor in the ambient air. The particle trace demonstrates significant deflection of streamlines toward the center axis, indicating an appreciable amount of air entrainment due to the buoyancy, thereby indicating the flow acceleration in the axis region. The middle layer is from the TiO_2 particles generated by the reaction with the water vapor from the combustion products. This clearly shows the rollup vortex structure, which is the source of the flame bulge.

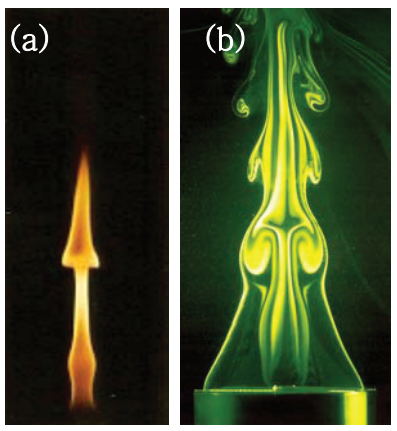

Fig. 1. Direct and RMS images of diffusion flame bulge in coflow.

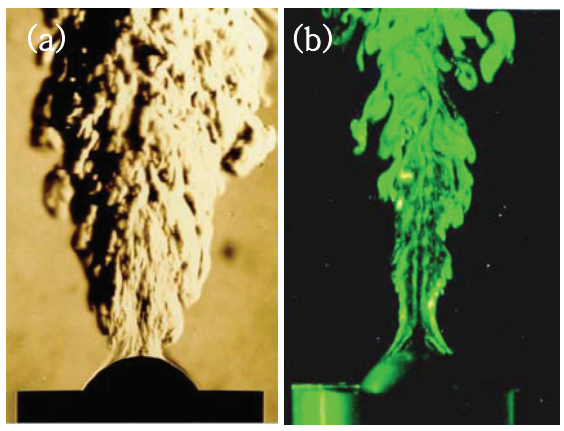

Fig. 2. Schlieren and RMS images of flame in curved-wall jet burner.

2.2 Axisymmetric Curved-Wall Jet Burner

There are several important factors in designing a burner, including flame stabilization, prevention of flashback, and flame size and control. Flame stabilization is related to burner safety and limits burner capacity. Prevention of flashback is important for safety in order to suppress unwanted explosion. Flame size is the limiting factor for combustor size, and its control is important for efficient heat transfer.

To simultaneously improve these characteristics, an axisymmetric curved-wall jet (CWJ) burner has recently been proposed (Gil et al., 1998). This burner utilizes the coanda effect by supplying fuel/air mixture through a slit around a half-sphere. Due to streamline curvature, the mixture initially adheres to the wall and, thus delaying flow separation. At a certain distance from the half-sphere, the flow separates and a recirculation zone is formed. On the ambient side, a large amount of air is entrained, resulting in a large spread angle of the jet. In the interaction region, the collision of the circular slit jet near the axis region generates a high level of turbulence.

To visualize the recirculation zone in the CWJ burner, the RMS technique has been applied. The results are shown in Fig. 2 together with the schlieren image. The schlieren image shows a large spread angle and strong turbulence structure, especially near the interaction jet region. The corresponding RMS image shows the recirculation zone above the half-sphere. Note that there exist large vortical structures along the outer boundary. Also, small vortical structures are developed near the centerline above the burner tip.

3. Flame Stabilization

3.1 Lifted Flame in Laminar Jets

Flame stabilization is one of the important issues related to the safety of practical burners. In this regard, liftoff and blowout phenomena have been extensively investigated for turbulent nonpremixed jet flames. However, there are still several competing theories by which to explain the turbulent lifted flame stabilization (Pitts, 1988).

As a first step to understanding the lifted flame stabilization mechanism, lifted flame behaviors in laminar jets have been investigated. It was observed that the base of a laminar lifted flame has a tribrachial (or triple) structure; a lean premixed flame (LPF), a rich premixed flame (RPF), and a diffusion flame (DF) coexist at the flame anchoring position, as shown in Fig. 3 (Chung and Lee, 1991; Lee et al., 1977). This flame structure suggests that the tribrachial point will be located along the stoichiometric contour of the jet, since all three types of flames coexist. Also, the flame base will have the propagation characteristics due to the existence of premixed flame wings at the edge. Since the tribrachial point is in stoichiometry, the propagation speed of a tribrachial flame S_{tri} is expected to be related to the stoichiometric laminar burning velocity $S_{L,st}$. Then, the flame stabilization mechanism would be the balance between S_{tri} and the local flow velocity along a stoichiometric contour.

The typical variation of liftoff height with jet velocity in laminar free jets is shown in Fig. 4, demonstrating that the liftoff height increases highly nonlinearly with jet velocity. Note that the liftoff height in turbulent jets increases linearly with jet velocity. The reason for the nonlinearity in laminar jets is explained in the following.

A typical direct photograph and a typical schlieren image for a laminar lifted flame, shown in Fig. 3, suggest that the flow upstream from the anchoring position can be reasonably approximated as a cold jet, since the typical premixed flame thickness is O (1 mm) while the liftoff height is O

(100 mm). Therefore, the flow field between the nozzle and flame base can be treated as a cold jet. By adopting the similarity solutions for the jet momentum and fuel species conservations, the axial velocity u and the fuel mass fraction Y_F can be derived as where, η is the similarity variable defined as $\sqrt{3/32}(u_0 d/\nu)(r/x)$, r and x are the radial and axial coordinates, respectively, ρ is the density, ν is the kinematic viscosity, J is the momentum flux at nozzle exit ($\pi\rho u_0^2 d^2/4$), I_F is the fuel mass flow rate ($\pi\rho u_0 d^2 Y_{F,0}/4$), d is the nozzle diameter, Sc_F is the Schmidt number of the fuel (ν/D_F), D_F is the mass diffusivity of fuel into air, and the subscript 0 indicates the condition at the nozzle exit.

$$u = \frac{3}{8\pi\nu x}\frac{J}{\rho}\frac{1}{\left(1+\eta^2/8\right)^2}, \qquad Y_F = \frac{\left(2\mathrm{Sc}_F+1\right)}{8\pi\nu x}\frac{I_F}{\rho}\frac{1}{\left(1+\eta^2/8\right)^{2\mathrm{Sc_F}}} \tag{1}$$

The tribrachial structure at the lifted flame base implies that when the flame is stabilized at the location of $\eta^*(x^*, r^*)$, it has stoichiometric concentration $Y_{F,st}$. Note that x^* is the liftoff height H_L. The axial flow velocity u^* at this point should balance the corresponding propagation speed of a tribrachial flame S_{tri}, which is assumed to be constant as a first approximation. By eliminating η^* from Eq. (1) and rearranging it, the following relations can be obtained (Chung and Lee, 1991; Lee et al., 1977):

$$\left(\frac{H_L}{d^2}\right)\left(\frac{\nu}{S_{tri}}\right) = \left(\frac{3}{32}\right)\left(\frac{3}{2\mathrm{Sc}_F+1}\frac{Y_{F,st}}{Y_{F,0}}\right)^{1/(\mathrm{Sc}_F-1)}\left(\frac{u_0}{S_{tri}}\right)^{(2\mathrm{Sc}_F-1)/(\mathrm{Sc}_F-1)} \tag{2}$$

Thus, the liftoff height relation for a specified fuel becomes

$$\left(\frac{H_L}{d^2}\right)\left(Y_{F,0}\right)^{1/(\mathrm{Sc}_F-1)} \propto u_0^{(2\mathrm{Sc}_F-1)/(\mathrm{Sc}_F-1)} = u_0^n \tag{3}$$

which shows that the liftoff height is proportional to the square of nozzle diameter and that the Schmidt number plays a crucial role for the dependence of jet velocity on liftoff height.

From the experiment in pure propane jets, the best fit as shown in Fig. 4 is for the velocity exponent of n = 4.733, with the corresponding Schmidt number of 1.37. This agrees well with the suggested Schmidt number of 1.376 for propane (Savas and Gollahalli, 1986). For n-butane jets, it is determined that n = 3.638 and Sc_F = 1.61 which agrees well with the suggested value of 1.524.

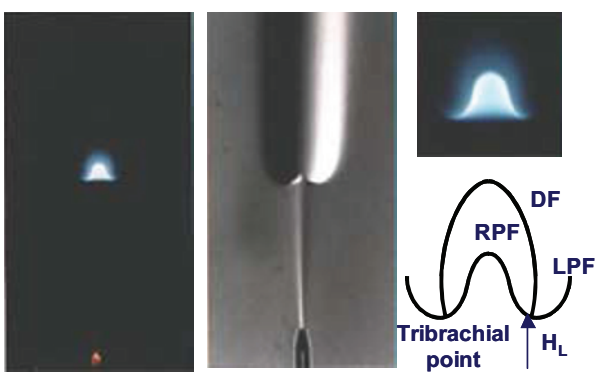

Fig. 3. Direct photograph, Schlieren photograph and schematic of a laminar lifted flame in a propane jet.

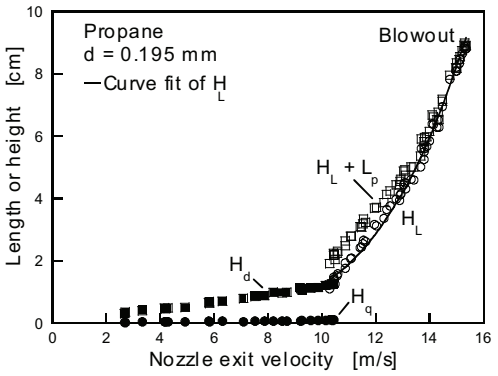

Fig. 4. Liftoff height with jet velocity.

Experiments in laminar free jets exhibited that lifted flames are observed for propane and n-butane fuels, while the nozzle attached flames in methane and ethane jets blow off directly without having lifted flames. The reason can be argued based on Eq. (3). The velocity exponent shows that the liftoff height decreases for $0.5 < Sc < 1$ (methane and ethane). The decrease in liftoff height with jet velocity is argued to be physically unrealistic. Later, it has been shown that the stabilization point is unstable for $Sc < 1$ in laminar free jets (Lee and Chung, 1997). Reattachment of lifted flames and blowout phenomena have also been investigated (Lee and Chung, 2001).

3.2 Lifted Flame in Turbulent Jets

It has been observed that there is a continuous transition from a laminar lifted flame to a turbulent lifted flame for the propane jet diluted with nitrogen, (Lee et al., 1994; Cha and Chung, 1996). Figure 5 shows the schlieren pictures of the lifted flames. The flame lifted off in the laminar regime (a) and its height increases nonlinearly with jet velocity. Then, the jet undergoes a breakup and the flame base is located downstream from the breakup height (b). Then, its height decreases with jet velocity. As the flow inside the nozzle undergoes a transition to turbulence near the Reynolds number of $Re_d \approx 2300$, the liftoff height decreases significantly (c). Finally, the liftoff height increases linearly with jet velocity in the turbulent regime (d).

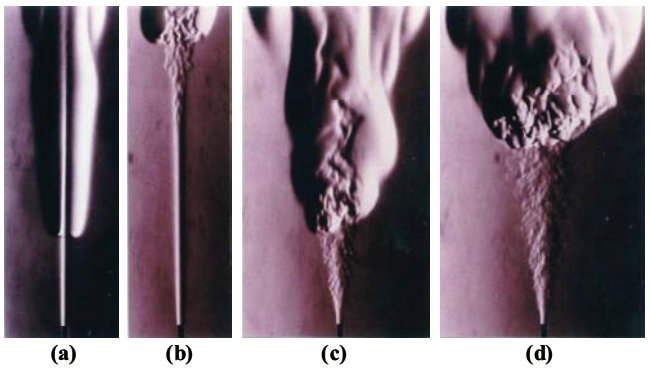

Fig. 5. Schlieren pictures demonstrating continuous transition from laminar to turbulent lifted flame with nitrogen diluted propane.

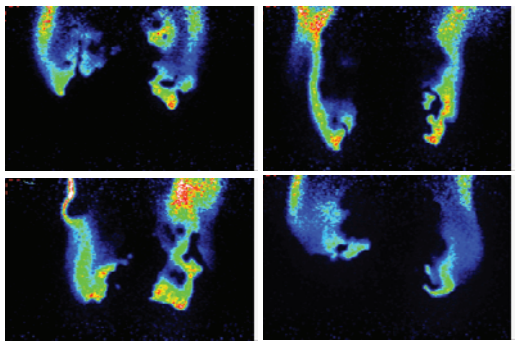

Fig. 6. Instantaneous images of OH PLIF at the base of a lifted flame in a turbulent jet at $Re_d = 26000$.

This continuous transition suggests that the tribrachial flame structure in the laminar regime can be related to the flame stabilization in the turbulent jet regime. Unlike the laminar regime, where the axisymmetric nature enables one to observe the tribrachial flame structure from the chemiluminescence, the turbulent flame base fluctuates. Thus, it is necessary to apply planar visualization techniques to identify the flame base structure.

3.3 Laser-induced Fluorescence

Planar OH LIF images at the bases of turbulent lifted flames for $d = 2.58$ mm and $Re_d = 26{,}000$ are shown in Fig. 6, demonstrating that it is difficult to identify the tribrachial structure from the OH PLIF images. To find a proper flame marker that can differentiate the tribrachial structure, laminar lifted flames have again been investigated by applying various diagnostic techniques, including OH and CH fluorescences and the chemiluminescence of OH* (Won et al., 2000). Figure 7 shows that CH PLIF and OH* can be an indicator of premixed flames and OH PLIF

can be an indicator of diffusion flames. Therefore, the combination of OH and either CH or OH* can be used to identify the tribrachial structure of turbulent lifted flame base. However, detailed study has not been performed yet.

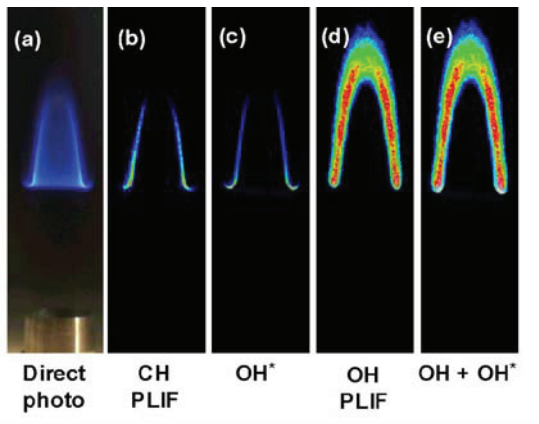

Fig. 7. Direct photo and various radical images for laminar lifted flame in coflow.

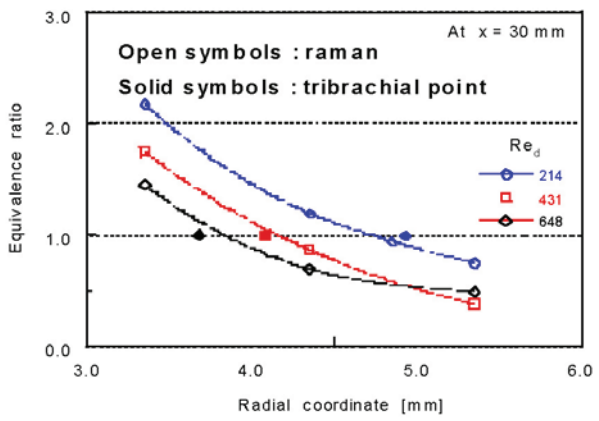

Fig. 8. Equivalence ratio in radial direction in laminar methane jet demonstrating stoichiometry at the tribrachial point.

3.4 Raman Scattering: Stoichiometric Concentration

In predicting the liftoff height characteristics in laminar jets, it has been assumed that the tribrachial flame is located along the stoichiometric contour. In order to experimentally verify this assumption, a spontaneous Raman scattering technique has been utilized (Ko et al., 2000). The local measurement results for laminar jets of methane are shown in Fig. 8 and are compared with the similarity solution. It also shows that the observed transient tribrachial points, which were determined from the trajectory of flame bases when ignited downstream, agree well with the measurements, such that the tribrachial flame is located along the stoichiometric contour. Fuel concentration field and flame characteristics are under investigation through Rayleigh scattering and CH* and OH PLIFs in laminar coflow jets, and one example of the visualization is shown in Fig. 9.

3.5 Lifted Flame in Coflow

In the studies of lifted flames in free jets, typical nozzle diameter d was O (0.1 cm) and jet velocity was O (100 cm/s). Tribrachial flame structures have also been observed in coflow jets with diluted fuel for $d = O$ (1 cm) and $U_0 = O$ (10 cm/s) (Plessing et al., 1998). For these free and coflow jets, the order of the Reynolds number $\mathrm{Re_d} = U_0 d/\nu$ remains relatively the same, while the Froude number, $\mathrm{Fr} = U_0^2/gd$, becomes three orders of magnitude smaller for coflows compared to free jets. Consequently, buoyancy can play an important role in influencing the flow field and thereby the lifted flame characteristics in the coflow.

Compared to free jet experiments, two interesting phenomena have been observed in coflows. One is that stationary lifted flames can be stabilized even when both the fuel jet and coflow velocities are smaller than the corresponding stoichiometric laminar burning velocity $S_{L,st}$. This is in contradiction to the balance mechanism between local flow velocity and the propagation speed of a tribrachial flame for lifted flame stabilization, since S_{tri} is larger than $S_{L,st}$ by the flow redirection effect (Reutch et al., 1995; Ko and Chung, 1999). The other interesting phenomenon was the

existence of periodically oscillating lifted flames with the frequency range of 2-5 Hz.

The flow visualization of a lifted flame in coflow with Mie scattering in normal gravity has been performed for both the cold flow of the diluted propane jet and the flow with lifted flame (Won et al., 2000). The cold flow field, as shown in Fig. 10, demonstrated the deceleration of axial momentum by the buoyancy due to heavy propane as compared to ambient air such that a stagnation region is formed. Then, the diluted propane flows radially and is carried downstream by coflow air. Consequently, the downstream part of the propane jet has a cylindrical fan shape. When a lifted flame is stabilized, the flow field becomes qualitatively different. The flow near the axis can be significantly accelerated by the buoyancy exerted on burnt gas. As a result, the diameter of the dark region near the lifted flame base is reduced significantly compared to the cold flow. Therefore, even though the nozzle exit velocity is smaller than the propagation speed of a tribrachial flame, the local axial velocity near the flame base will be significantly accelerated such that the validity of the balance mechanism of the local flow velocity and the propagation speed for a lifted flame stabilization can be maintained.

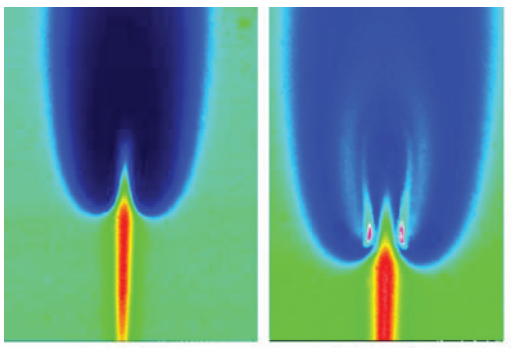

Fig. 9. Rayleigh image demonstrating fuel concentration and burnt region together with CH^* and OH PLIF images.

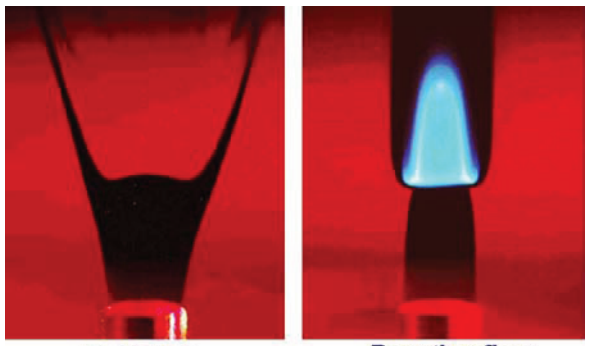

Fig. 10. Mie scattering images of cold and reacting flows demonstrating entrainment by buoyancy.

3.6 Lifted Flame Oscillation

At a certain range of jet velocity and fuel dilution, oscillating lifted flames were observed in the coflow. The oscillating mechanism has been attributed to the buoyancy driven instability (Kim et al., 2002). When the flame migrates upstream (downstream), the flame encounters effectively higher (lower) flux of fuel, thus burning rate increases (decreases). This increases (decreases) buoyancy and, consequently, local velocity. As a result, the flame migrates downstream (upstream). This repetitive interaction of burning rate and buoyancy-induced convection has been attributed to the lifted flame oscillation.

To characterize this, OH and acetone fluorescence techniques were applied to visualize the flame and fuel concentration field (Won et al., 2002). Figure 11 shows the results demonstrating the variation in flame size, which characterizes burning rate. During the flame oscillation, the fuel concentration field varies significantly. For example, when the flame base is propagating upstream (falling period), the concentration field is much more flattened compared to the rising period. This is an indication of the variation in concentration field due to air entrainment by the buoyancy.

The buoyancy driven instability mechanism has been tested by conducting experiments at

the Japan Microgravity Center (JAMIC) to eliminate the buoyancy effect, where the 10 s microgravity condition can be obtained. Figure 12 shows the sequence of photographs after the drop in microgravity experiment for the oscillating flame in normal gravity. The results demonstrate that the flame becomes completely stationary, when the buoyancy is absent, substantiating again the effect of buoyancy on the flame oscillation.

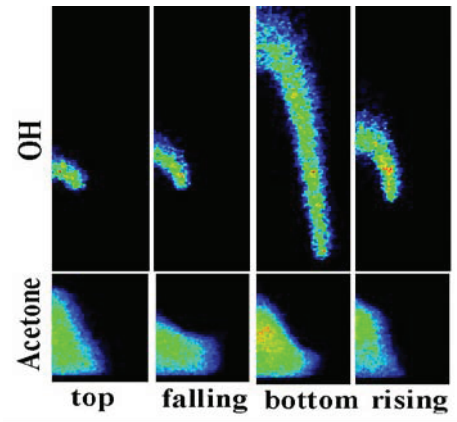

Fig. 11. OH and acetone fluorescences demonstrating burning rate and concentration field during oscillation.

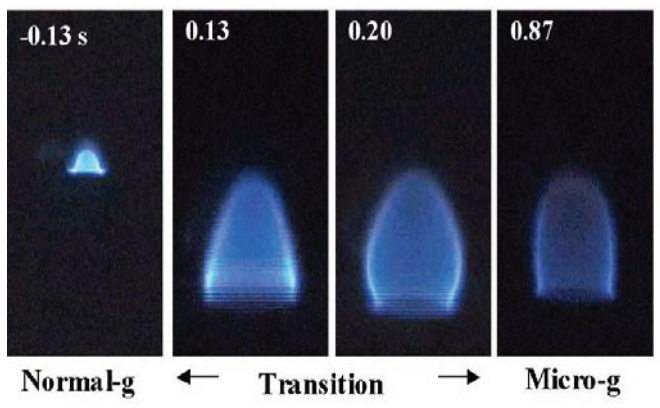

Fig. 12. Variation of flame shape after drop in microgravity experiment.

4. Vortex Visualization

Since turbulent flow is composed of many wormlike structures of vortex tubes, one of the interesting phenomena related to turbulent combustion can be the flame propagation along a vortex. In this regard, many studies have been focused on the flame propagation along a vortex tube for premixed systems. Considering the importance of nonpremixed combustion, where the vortex structures can be easily formed in the mixing layer of fuel and oxidizer, the flame propagation along a nonpremixed vortex tube has been investigated recently (Choi et al., 1999). A vortex ring of propane fuel was generated by the single stroke motion of a speaker. The vortex ring was ejected out of a tube nozzle with the diameter of 5 cm and was ignited at the center of the vortex ring by focusing a Nd:YAG laser to minimize the flow disturbance associated with igniters.

The propagating flame was visualized by an intensified charge-coupled device (ICCD) camera. A series of direct photographs demonstrating the side (a), top (b), and front (c) views is shown in Fig. 13. It is interesting to note that the front view of the flame is circular at 18 ms, which corresponds to the timing when the flame propagated 90° from the ignition point. Also, the side view shows that the maximum intensities occur off the center axis. These characteristics imply that the flame front shape is a circular ring.

To further illustrate the flow field, a trace amount of acetone is added to the fuel stream and the LIF technique was applied to visualize the vortex (Choi et al., 2002). Figure 14 shows the spiral ring region of the vortex ring and the corresponding front view of the flame. The results demonstrate that the diameter of the flame having maximum intensity is comparable to the diameter of the innermost spiral ring. This suggests that the flame is propagating through a region with an appreciable concentration gradient, thus demonstrating the possibility of the flame front having a tribrachial structure.

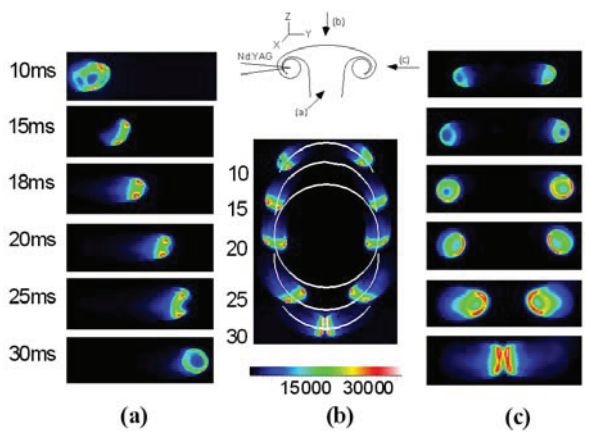

Fig. 13. ICCD images of flame propagation along a nonpremixed vortex tube: (a) side, (b) top, and (c) front view.

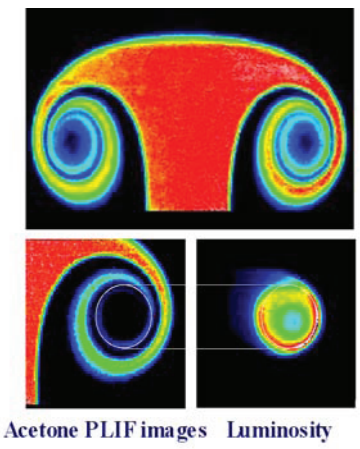

Fig. 14. Acetone PLIF for fuel concentration field and direct photo of propagating flame in a vortex tube.

5. Soot Zone Structure

Soot formation and control in diffusion flames are important for industrial burners for proper radiation heat transfer and for the environment. Frequently adopted flow systems in fundamental studies on soot are coflow and counterflow. Note that the counterflow flame can be a model for turbulent diffusion flames in the laminar flamelet model.

Generally, soot is formed on the fuel side of a diffusion flame. In coflow flames, when the flame surrounds the whole fuel (oxidizer) zone, it is called a normal (inverse) diffusion flame (NDF(IDF)). For a normal diffusion flame with pure fuel and air, soot is formed on the fuel side and then is oxidized when passing through the flame by the streamline characteristics (soot formation/oxidation flame: SFO). If such a diffusion flame is stabilized in a counterflow, the flame is located on the oxidizer side due to the stoichiometry, as schematically shown in Fig. 16. In such a situation, when soot particles are formed, they will follow the streamline such that the particles cannot pass through the flame, and rather will be carried away through the stagnation plane without occurrence of the soot oxidation process (soot formation flame: SF). Therefore, the counterflow flame cannot adequately describe the soot characteristics of the normal diffusion flame when pure fuel and air are used. Note that when the flame is located on the fuel side in counterflow, the soot particles generated on the fuel side can be oxidized. Therefore, similarity in soot characteristics exists between normal (inverse) diffusion flame in coflow and a counterflow flame when the flame is located on the fuel (oxidizer) side, both of which are soot formation/oxidation (soot formation) flames (Kang et al., 1997; Hwang and Chung, 2001).

The soot characteristics in counterflow diffusion flames were visualized using a sheet beam from an Ar-ion laser (Fig. 15) to visualize the soot zone from Mie scattering together with the chemiluminescence of flame in a counterflow. For the soot formation flame with the flame located on the oxidizer side, the Mie scattering image shows that soot particles leaked through the stagnation plane and formed a large recirculation zone outside of the oxidizer stream, which is supplied from the top. Thus, soot oxidation is absent. For the soot formation/oxidation flame, the flame structure demonstrates that soot particles formed on the fuel side do not leak and are oxidized.

Soot zone structures can be further analyzed by adopting laser extinction and scattering techniques. An example is exhibited in Fig. 16. A direct photograph of a normal coflow diffusion flame, laser extinction and scattering signals are shown. Since the extinction signal is the accumulation of line-of-sight information, the signal is Abel transformed to represent local information of soot volume fraction. By using the soot volume fraction and scattering signal, soot volume fraction, diameter, and number density can be determined. The laser-induced incandescence (LII) technique has also been applied for soot structure studies, which again represents soot volume fraction. The advantage of LII is that instantaneous measurement is possible.

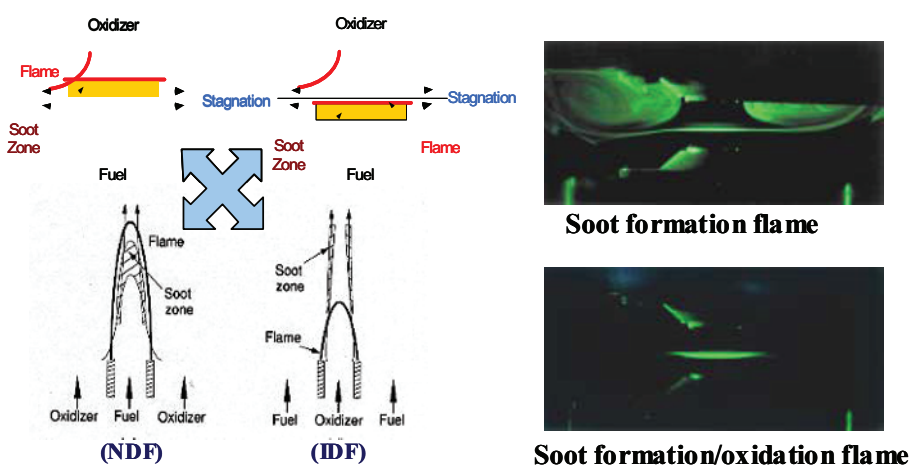

Fig. 15. Schematic diagram showing soot zone and streamline for counterflow and coflow diffusion flames and visualization of soot zone.

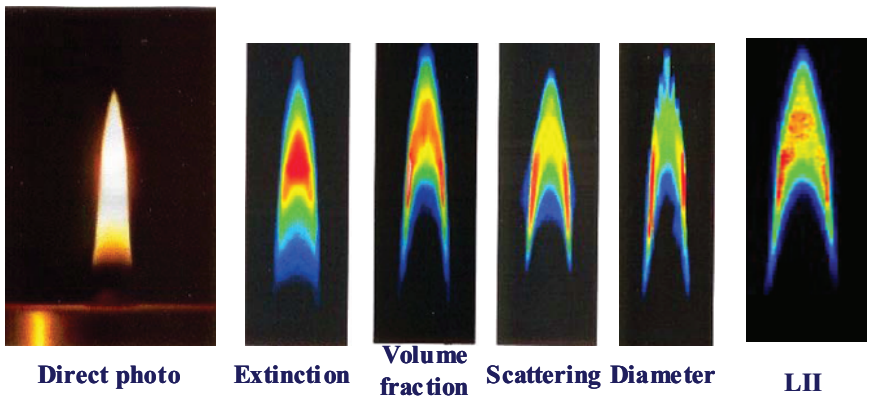

Fig. 16. Soot extinction and scattering images representing volume fraction and diameter for coflow diffusion flame together with LII.

6. Concluding Remarks

Various visualization techniques have been applied to enhance the understanding of combustion phenomena. These include flow visualization using reactive Mie scattering and acetone fluorescence, concentration measurements from Raman and Rayleigh scatterings, radical distributions using OH and CH planar laser-induced fluorescence, and soot zone structure from laser light extinction and scattering and laser-induced incandescence. These combustion diagnostics can identify the mechanisms involving the flame bulge formation through vortex

formation in coflow diffusion flames, the existence of a recirculation zone on top of the curved-wall jet burner, the tribrachial flame structure at the base of a laminar lifted flame, the oscillation mechanism of the lifted flame in coflow, the flame propagation along a nonpremixed vortex ring, and soot zone structures in counterflow and coflow diffusion flames. These demonstrated the usefulness of laser diagnostics tools in the visualization of combustion phenomena.

Acknowledgments

This work was supported by the Combustion Engineering Research Center. Contributions by Prof. B. J. Lee, Drs. M. S. Cha, Y. S. Gil, J. Y. Hwang, K. T. Kang, Y. S. Ko, and J. S. Lee are greatly appreciated.

References

Cha, M. S. and Chung, S. H., Characteristics of Lifted Flames in Nonpremixed Turbulent Confined Jets, *Proc. of Combust. Inst.*, 26(1996), 121-128.

Choi, H. J., Ko, Y. S. and Chung, S. H., Flame Propagation along a Nonpremixed Vortex Ring, *Combust. Sci. Tech.,* 139(1998), 277-292.

Choi, H. J., Ko, Y. S. and Chung, S. H., Visualization of Concentration Field in a Vortex Ring using Acetone PLIF, to appear in *J. Visualization*, 5-2(2002).

Chung, S. H. and Lee, B. J., On the Characteristics of Laminar Lifted Flames in Nonpremixed Jet, *Combust. Flame*, 86(1991), 62-72.

Eckbreth, A. C., Laser Diagnostics for Combustion Temperature and Species, 2nd Ed., Gordon and Breach, Amsterdam, (1996).

Gil, Y. S., Jung, H. S. and Chung, S. H., Premixed Flame Stabilization in an Axisymmetric Curved Wall Jet, *Combust. Flame*, 113(1998), 348-357.

Hwang, J. Y. and Chung, S. H., Growth of Soot Particles in Counterflow Diffusion Flames of Ethylene, *Combust. Flame,* 125(2001), 752-762.

Kang, K. T., Hwang, J. Y., Chung, S. H. and Lee, W., Soot Zone Structure and Sooting Limit in Diffusion Flames: Comparison of Counterflow and Coflow Flames, *Combust. Flame*, 109(1997), 266-281.

Kim, J., Won, S. H., Shin, M. K. and Chung, S. H., Numerical Simulation of Oscillating Lifted Flames in Coflow Jets with Highly Diluted Propane, to appear in *Proc. of Combust. Inst.*, 29 (2002).

Ko, Y. S. and Chung, S. H., Propagation of Unsteady Tribrachial Flames in Laminar Nonpremixed Jets, *Combust. Flame,* 118(1999), 151-163.

Ko, Y. S., Chung, S. H., Kim, G. S. and Kim, S. W., Stoichiometry at the Leading Edge of a Tribrachial Flame in Laminar Jets from Raman Scattering Technique, *Combust. Flame,* 123(2000), 430-433.

Lee, B. J., Cha, M. S. and Chung, S. H., Characteristics of Laminar Lifted Flames in a Partially Premixed Jet, *Combust. Sci. Technol.* 127(1997), 55-70.

Lee, B. J. and Chung, S. H., Stabilization of Lifted Flames in a Laminar Nonpremixed Jet, *Combust. Flame*, 109(1997), 163-172.

Lee, J. S. and Chung, S. H., Characteristics of Reattachment and Blowout of Laminar Lifted Flames in Partially Premixed Propane Jets, *Combust. Flame*, 127(2001), 2194-2204.

Lee, H. H., Hwang, J. Y., Chung, S. H. and Lee, W., Visualization and Control of Buoyant Diffusion Flames with Periodic Fuel Supply, 8th International Symposium on Flow Visualization, *Proc. of 8th International Symposium on Flow Visualization*, Sorrento, Italy 55 (1998), 1-8

Lee, B. J., Kim, J. S. and Chung, S. H., Effect of Dilution on the Liftoff of Nonpremixed Jet Flames, *Proc. of Combust. Inst.*, 25(1994), 1175-1181.

Pitts, W. M., Assessment of Theories for the Behavior and Blowout of Lifted Turbulent Jet Diffusion Flames, *Proc. of Combust. Inst.*, 22(1988), 809-816.

Plessing, T., Terhoeven, P., Peters, N. and Mansour, M. S., An Experimental and Numerical Study of a Laminar Triple Flame, *Combust. Flame,* 115(1998), 335-353.

Reutch, G. R., Vervisch, L. and Liñán, A., Effects of Heat Release on Triple Flame, *Phys. Fluids,* 7(1995), 1447-1454.

Savas, Ö. and Gollahalli, S. R., Stability of Laminar Round Gas-jet Flame, *J. Fluid Mech.*, 165(1986), 297-318.

Won, S. H., Cha, M. S., Chung, S. H. and Lee, B. J., Lifted Flame Stabilization in Developing and Developed Regions of Coflow Jets for Highly Diluted Propane, *Proc. of Combust. Inst.*, 28(2000), 2093-2099.

Won, S. H., Kim, J., Shin, M. K. and Chung, S. H., Fujita, O., Mori, T., Choi, J. H., and Ito, K., Normal and Micro Gravity Experiment of Oscillating Lifted Flames in Coflow, to appear in *Proc. of Combust. Inst.*, 29(2002).

Author Profile

Suk Ho Chung: He received his B.S. degree in Mechanical Engineering in 1976 from Seoul National University, and his Ph.D. degree in Mechanical Engineering in 1983 from Northwestern University. He is a professor since 1984 in the School of Mechanical Engineering, Seoul National University. His research interests cover combustion fundamentals, pollutant formation, and laser diagnostics.